Analysis of Soft Fibers with Kinematic Constraints and Cross-Links by Finite Deformation Beam Theory

Franck Vernerey[1] and Ronald Y. S. Pak[2]

Abstract: This paper presents a hybrid analytical–computational mechanics formulation for an arbitrarily curved Timoshenko beam undergoing planar finite deformation and subjected to kinematic constraints in the form of fixed displacement and cross-linking. On the basis of an analytical reduction of the governing equations, the system reduced to a single nonlinear differential equation coupled with integral equations associated with translational constraints. An effective numerical formulation of the problem with general distributed and pointwise constraints is shown to be possible by using a simple finite-element procedure. To illustrate the efficiency and accuracy of the method, several examples are introduced to study both stable and bifurcation problems and a system of interacting fibers with different types of cross-link constraints. Because of the reduction of discretization error and the dimension of the matrix system, the proposed formulation is likely to be an attractive computational platform for modeling large-scale multifiber problems, as in fibrous microstructure simulations and other applications. **DOI: 10.1061/(ASCE)EM.1943-7889.0000256.**

CE Database subject headings: Fibers; Beams; Structures; Kinematics; Deformation.

Author keywords: Flexible fibers; Fibrous networks; Beams; Structures; Cross-links; Large deformation.

Introduction

The theoretical study of fibrous networks is becoming a increasingly active research topic because of its strong relevance to bioengineering, cell mechanics, and material science. Fibrous networks are usually characterized by a very large number of fibers interacting through cross-linkage and contact. Because of their slender shape, fibers can generally be modeled by either the Bernoulli beam theory (if the distance between cross-links is large compared to the fiber radius) or the Timoshenko beam theory (if the distance between cross-links becomes comparable to the fiber radius). The finite deformation of a slender fiber with finite stiffness in stretching, shear, and flexure has been an active research topic in the structural mechanics community in the context of beam theories because of its relevance to numerous applications in civil, aerospace, and mechanical engineering. Several routes have been undertaken to study these problems. For simple beam geometries, for example, exact analytical solution have been derived (DaDeppo and Schmidt 1969; Lau 1982; Goto et al. 1990), which provided a fundamental understanding of the behavior of beams and columns undergoing finite deformation (Irschik and Gerstmayr 2009). They also serve well as important benchmarks against which approximate or numerical solutions can be evaluated. For more complex shapes and loading conditions, however, numerical methods are a necessity. To this end, a number of discretization methods have been proposed in the literature. Examples are finite-difference methods (Huddleston 1968) and finite-element methods (Kapania 1986; Simo 1985; Simo and Vu-Quoc 1986). Many related issues, including bifurcation points (Schmidt and DaDeppo 1972; Knight and Carron 1997), snap-through instabilities (Simo and Vu-Quoc 1986) and postbuckling behavior (Ricks 1972) have been advanced for general beam configurations. Because of the cumulative error effects in common numerical discretization procedures and the nonlinear nature of the finite deformation problem, many proposed solutions are unfortunately limited in accuracy and reliability relative to the computational efforts required.

To reduce the solution errors, hybrid analytical-computational formulations (Saje 1990, 1991; Pak and Stauffer 1994) have proven to have serious potential. For planar deformation, for example, it has been shown that the analysis of the three nonlinear, coupled, governing differential equations corresponding to the two displacements and one rotation field for the beam can be effectively reduced to only one (Saje 1990, 1991; Pak and Stauffer 1994). Although it constitutes a powerful conceptual basis for accurate and efficient numerical formulations, the approach is currently limited to specific loading and constraint conditions. This is a critical obstacle to the modeling of a large assembly of fibers with arbitrary interactions. In this paper, the more complicated problem of single or multiple fibers subject to pointwise kinematic constraints under finite displacements is attempted by using the hybrid method. By expressing the relationships among displacement, force, and beam orientation in the form of an integral equation, two common types of constraints are considered: fixed displacement and cross-link interactions (enforcing that two points must undergo the same displacement). It will be shown that the resulting coupled differential-integral equation formulation so derived can be readily solved numerically by using one-dimensional (1D) finite-element methods. The proposed generalization of the finite beam formulation permits the consideration of a large variety of problems with the accuracy and elegance of the theories of elastica (Saje 1990, 1991; Pak and Stauffer 1994). The proposed method also naturally provides an attractive platform for large-scale, nonlinear, multifiber

[1]Assistant Professor, Dept. of Civil, Environmental, Architectural Engineering, Univ. of Colorado at Boulder, 1111 Engineering Dr. 428, UCB, ECOT 422, Boulder, CO 80309-0428 (corresponding author). E-mail: franck.vernerey@colorado.edu

[2]Professor, Dept. of Civil, Environmental, Architectural Engineering, Univ. of Colorado at Boulder, 1111 Engineering Dr. 428, UCB, Boulder, CO 80309-0428.

Note. This manuscript was submitted on May 27, 2010; approved on February 22, 2011; published online on February 24, 2011. Discussion period open until January 1, 2012; separate discussions must be submitted for individual papers. This paper is part of the ***Journal of Engineering Mechanics***, Vol. 137, No. 8, August 1, 2011. ©ASCE, ISSN 0733-9399/2011/8-527–536/$25.00.

problems of serious interest not only to biomechanics, but also to structural mechanics and many related modern engineering disciplines. The paper is organized as follows. In the following section, the kinematic assumptions and governing conditions for the finite deformation of beams are laid out. The next section describes the resulting analytical framework and derives the equations for the study of elastic beams. After that, the integral equations for applying kinematic constraints, focusing of fixed displacement, and cross-link interactions are introduced. Then the finite-element computational formulation is introduced, and a set of examples illustrating the capability and performance of the formulation are presented. The final section presents the conclusions.

Fundamental Governing Equations

Kinematics

With the basic assumption of plane sections remaining plane and allowing for axial, flexural, and shear deformations as in the classical Timoshenko beam theory, the basic elements of the proposed 1D finite deformation mechanics formulation for a curvilinear beam are shown in Fig. 1. A material point $\mathbf{X}$ in the initial configuration C_X of the beam is taken to have the Cartesian coordinates (X_1, X_2) with respect to a fixed frame and the orthogonal curvilinear coordinates (s, n) defined by using the initial centroidal line of the beam. Its image $\mathbf{x}$ in the deformed configuration C_x is denoted by the Cartesian coordinates (x_1, x_2) and convected coordinates $(\tilde{s}, \tilde{n})$, which correspond to the directions of (s, n) after deformation. Accordingly, the displacement vector $\mathbf{u}$ of a point $\mathbf{X}$ can be defined by its Cartesian components $(u_1, u_2) = (x_1, x_2) - (X_1, X_2)$. Similarly, the orientation of an arbitrary cross-sectional plane of the beam in its initial configuration C_X with respect to the vertical X_2-axis is expressed in terms of the angle ϕ_0 and its image in the current configuration C_x by ϕ. As the angular difference between the direction of $\tilde{n}$ and the orientation of the normal to the deformed centroidal axis (see Fig. 1), the shear deformation is measured by

$$\alpha = \phi - \beta \tag{1}$$

where β = angle between the normal to the centroid and the vertical axis in the current configuration (Fig. 1). For describing the longitudinal stretch at any point of the beam, a scalar measure e, which gives the current length of a differential beam element as $(1 + e)ds$, is equally useful. In terms of the foregoing notations

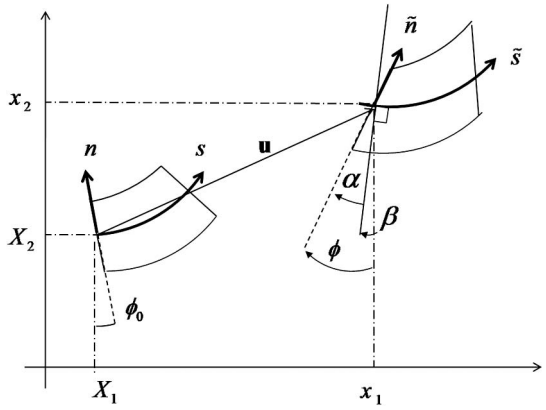

Fig. 1. Free-body diagram of a beam cross section in initial and current configurations

$$\mathbf{X}' = \begin{bmatrix} \cos\phi_0(s) \\ \sin\phi_0(s) \end{bmatrix} \quad \text{and} \quad \mathbf{x}' = (1+e)\begin{bmatrix} \cos\beta(s) \\ \sin\beta(s) \end{bmatrix} \tag{2}$$

as their Cartesian components, with the prime denoting differentiation with respect to the arc-length coordinate s. From these kinematic definitions, it can be shown that, for small to moderate values of e, α, and $(\phi' - \phi_0')$, the Green-Lagrange strain tensor $\hat{\mathbf{E}}$ evaluated in the beam cross section is approximated by (Pak and Stauffer 1994)

$$\hat{\mathbf{E}} \approx \frac{R_0}{R_0 - Y_2}\begin{bmatrix} \epsilon - Y_2\kappa & \gamma/2 \\ \gamma/2 & 0 \end{bmatrix} \tag{3}$$

where Y_2 = section coordinate in the $\mathbf{n}$ direction (in the reference configuration) and

$$\epsilon = (1+e)\cos\alpha - 1, \qquad \gamma = (1+e)\sin\alpha, \qquad \kappa = \phi' - \phi_0' \tag{4}$$

In the preceding equation, $R_0 = 1/\phi_0'$ = initial radius of curvature; and ϵ, γ, and κ = fundamental scalar measures of the stretch, shear, and bending deformations, respectively, in the 1D beam mechanics formulation used in this paper.

Equilibrium Equations and Boundary Conditions

Following the kinematic assumptions stated in the preceding section, the theorem of virtual work may be invoked. It states

$$\delta W_{\text{int}} - \delta W_{\text{ext}} = 0 \tag{5}$$

where δW_{int} and δW_{ext} = virtual work done by the internal and external forces, respectively. Using the initial configuration C_X as the reference configuration for the problem depicted in Fig. 2, δW_{int} and δW_{ext} may be written in the following form:

$$\delta W_{\text{int}} = \int_0^{L_0} (P\delta\epsilon + V\delta\gamma + M\delta\kappa)ds \tag{6}$$

$$\delta W_{\text{ext}} = \int_0^{L_0} (\mathbf{p}\cdot\delta\mathbf{u} + \mu\delta\phi)ds + \sum_{j=1}^{N} [\mathbf{f}^j\cdot\delta\mathbf{u} + m^j\delta\phi]_{s=s^j} \tag{7}$$

where L_0 = initial length of the beam; P, V, and M = resultants of the axial stress, shear stress, and bending moment with respect to the initial configuration; $\mathbf{p}(s) = (p_1, p_2)$ and $\mu(s)$ = rectangular components of the externally applied distributed force and moment resultants, respectively, along the beam; and $\mathbf{f}^j = (f_1^j, f_2^j)$ and m^j = concentrated forces and moment prescribed at selected locations $s = s^j$, $j = 1, \ldots, N$ along the beam likewise. Upon an integration by parts and a substitution of the strain definitions of Eq. (3) in Eqs. (5)–(7), three nonlinear ordinary differential equations can be derived from the variational principle of Eq. (5):

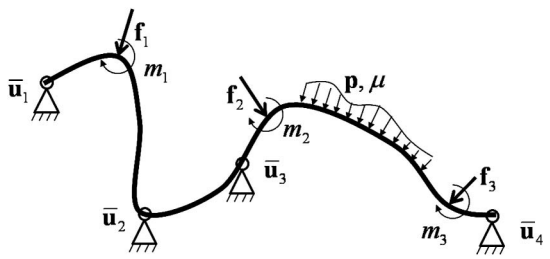

Fig. 2. Forces and kinematic constraints applied to the beam

J. Eng. Mech., 2011, 137(8): 527-536

$$\left\{\begin{array}{rcl}(\mathbf{R}\cdot\boldsymbol{\Xi})' & = & \mathbf{p}\\ M'-\mathbf{e}:(\boldsymbol{\Xi}\otimes\boldsymbol{\Pi}) & = & \mu\end{array}\right\},\quad s\in(0,L)-\{s_j,j=1,\ldots,N\} \tag{8}$$

where the vectors $\boldsymbol{\Xi}$ and $\boldsymbol{\Pi}$ = measures of axial and shear stress and strain, respectively:

$$\boldsymbol{\Xi}=\begin{bmatrix}P\\V\end{bmatrix}\quad\text{and}\quad\boldsymbol{\Pi}=\begin{bmatrix}\epsilon+1\\\gamma\end{bmatrix} \tag{9}$$

whereas $\mathbf{e}$ = permutation tensor; $\mathbf{R}$ = orthogonal rotation matrix; and $\mathbf{w}$ = orientation vector given by

$$\mathbf{e}=\begin{bmatrix}0&-1\\1&0\end{bmatrix},\quad\text{and}\quad\mathbf{R}(\phi)=\begin{bmatrix}\cos\phi&-\sin\phi\\\sin\phi&\cos\phi\end{bmatrix} \tag{10}$$

The conditions for a set of prescribed concentrated forces/moments or displacements/rotation at discrete points along the beam also translate to

$$\left\{\begin{array}{rcl}[\mathbf{R}\cdot\boldsymbol{\Xi}](s^j) & = & \mathbf{f}^j\\ [M](s^j) & = & m^j\end{array}\right\}j=1,\ldots,q\quad\text{and}\quad\left\{\begin{array}{rcl}\mathbf{u}(s^j) & = & \bar{\mathbf{u}}^j\\ \phi(s^j) & = & \bar{\phi}^j\end{array}\right\}j=(q+1),\ldots,(q+r) \tag{11}$$

where the square brackets $[\,]$ denote the jump across s^j in the encapsulated quantity; and q and r = number of points at which a concentrated force/moment and prescribed displacement/rotation are applied, respectively.

To cater to a sufficiently wide range of applications, two kinds of external loading will be considered in this formulation: conservative and nonconservative "follower" loads. Both kinds of loads may occur in the form of concentrated actions $\mathbf{f}^j$ at certain points $s=s^j$ or distributed forces $\mathbf{p}$ along the entire beam. To this end, $\bar{\mathbf{f}}^j$ and $\bar{\mathbf{p}}$ are used to denote the concentrated and distributed conservative forces whose directions and magnitude do not depend on the beam's deformation. With a focus on follower forces whose directions remain constant with respect to a coordinate system that rotates with the beam centroidal axis (e.g., fluid pressure loading whose direction always remains perpendicular to the contact surface), their distributed and concentrated components $\tilde{\mathbf{p}}$ and $\tilde{\mathbf{f}}^j$ are written as

$$\tilde{\mathbf{p}}^G(\phi)=\mathbf{R}(\phi)\cdot\tilde{\mathbf{p}}\quad\text{and}\quad(\tilde{\mathbf{f}}^j)^G(\phi_j)=\mathbf{R}(\phi_j)\cdot\tilde{\mathbf{f}}^j \tag{12}$$

where the superscript G denotes vectors in the fixed global Cartesian coordinate system X_i; and $\mathbf{R}$ = orthogonal rotation matrix defined in Eq. (10). As the resultant of both conservative and follower forces, the total external load vectors in Eqs. (8) and (11) can be expressed compactly as

$$\mathbf{p}=\bar{\mathbf{p}}+\mathbf{R}(\phi)\cdot\tilde{\mathbf{p}} \tag{13}$$

$$\mathbf{f}^j=\bar{\mathbf{f}}^j+\mathbf{R}(\phi_j)\cdot\tilde{\mathbf{f}}^j \tag{14}$$

where $\phi_j=\phi(s^j)$ and the arguments s and s^j are omitted for brevity.

Constitutive Relation

To complete the mechanical formulation, a set of constitutive relations are needed to describe the mechanical response of the beam. For many engineering applications, the class of nonlinear hyperelastic beam whose mechanical behavior can be entirely defined by a hyperelastic potential $\Psi(\epsilon,\gamma,\kappa)$ is of interest. Representing the stored elastic energy in the beam cross section, Ψ can be related to the stress resultant by

$$[P\quad V\quad M]=\left[\Psi_{,\epsilon}\quad\Psi_{,\gamma}\quad\Psi_{,\kappa}\right] \tag{15}$$

where the commas denote partial differentiation. For instance, in the case of a linear relationship between the deformation measures and their corresponding cross-sectional stress resultants, the elastic potential Ψ can be written as

$$\Psi(\epsilon,\gamma,\kappa)=\frac{EA}{2}\epsilon^2+\frac{kGA}{2}\gamma^2+\frac{EI}{2}\kappa^2 \tag{16}$$

where E and G = Young's and shear moduli, respectively; A and I = area and moment of inertia of the beam cross section; and k = factor representing the effective shear modulus of the beam to allow for the nonuniform cross-sectional shear stress distribution. Although the general case of a nonlinear elastic beam can be considered, this study concentrates on the case of linear elasticity for the sake of clarity.

Reduction of System of Governing Equations

To achieve an analytical reduction of the equation system in Eqs. (8)–(11) for higher mathematical and computational efficiency, it is useful to note that the stress resultant Eq. (8) can be integrated to give an expression for the components (P,V) of the vector $\boldsymbol{\Xi}$ in terms of external forces. Because $\mathbf{R}$ is an orthogonal tensor, $\boldsymbol{\Xi}$ can be written as

$$\boldsymbol{\Xi}=\mathbf{R}^T\cdot\mathbf{F}\quad\text{where }\mathbf{F}(s)=\sum_{j=0}^{\eta(s)}\mathbf{f}^j(s^j)+\int_0^s\mathbf{p}(s)ds \tag{17}$$

and $\eta(s)$ = integer function defined by

$$\eta=\begin{cases}0 & \text{if } s<s_1\\ j & \text{if } s\in[s^j,s_{j+1})\\ N & \text{if } s\geq s_N\end{cases} \tag{18}$$

where N = number of concentrated forces along the beam. Eq. (17) gives a direct relationship between axial and shear stress resultants in the beam in terms of the imposed external forces.

Reduced Equilibrium Equation

When there are no translational kinematic constraints applied on a beam (the displacement of any point along the beam is not constrained in any way), it is possible to decouple the moment and force equations. Thus, following the formulation described in Saje (1990, 1991) and Pak and Stauffer (1994), the system of Eq. (8) can be reduced to a single ordinary differential equation for ϕ. The displacement may thus be recovered through a simple integration along the beam. The reduction of the system is explained as follows. Starting from the moment equation in Eq. (8), it is useful to introduce the function $g(\mathbf{F},\phi)$ defined as

$$g(\mathbf{F},\phi)=-\mathbf{e}:(\boldsymbol{\Xi}\otimes\boldsymbol{\Pi})-\mu=\mathbf{e}:(\mathbf{w}\otimes\mathbf{F})+\lambda_1\mathbf{F}\cdot\mathbf{P}_1\cdot\mathbf{F}-\mu \tag{19}$$

where the last equality only holds in case of linear elasticity introduced previously. The matrix $\mathbf{P}_1$, orientation vector $\mathbf{w}$, and material constant λ_1 appearing in Eq. (21) are given by

J. Eng. Mech., 2011, 137(8): 527-536

$$\mathbf{P}_1 = \begin{bmatrix} -\sin 2\phi & \cos 2\phi \\ \cos 2\phi & \sin 2\phi \end{bmatrix}, \quad \mathbf{w}(\phi) = \begin{bmatrix} \cos\phi \\ \sin\phi \end{bmatrix}, \quad \text{and} \quad \lambda_1 = \frac{1}{2}\left(\frac{1}{EA} - \frac{1}{kGA}\right) \tag{20}$$

Using these definitions and the linear relationship between moment and curvature $\phi' - \phi'_0$, the moment equation in Eq. (8) is written in the simple form

$$EI(\phi' - \phi'_0) + g(\mathbf{F}, \phi) = 0 \tag{21}$$

Together with the boundary and jump conditions

$$\begin{cases} [\Psi^*_{,\kappa}\phi(s^j)] = m^j & j = 1, \ldots, q \\ \phi(s^j) = \bar{\phi}^j & j = (q+1), \ldots, (q+r) \end{cases} \tag{22}$$

analogous to Neumann- and Dirichlet-type boundary conditions, respectively, Eq. (21) constitutes the basic equation to be solved for a complete characterization of the problem.

Displacement-Rotation Relation

As the axial and shear stress resultants are defined in terms of ϕ, the displaced position $\mathbf{x}$ of a material point as $\mathbf{X} + \mathbf{u}$ along the centroidal axis of the beam may be determined by direct integration. Once again, it is useful to define a function $\mathbf{q}(\mathbf{F}, \phi)$ as follows:

$$\mathbf{q}(\mathbf{F}, \phi) = (1+e)\begin{bmatrix} \cos\beta \\ \sin\beta \end{bmatrix} = \mathbf{R}\cdot\mathbf{\Pi} = \mathbf{w} + \mathbf{P}_2 \cdot \mathbf{F} \tag{23}$$

where the last equality is obtained by using the linear elasticity assumption and

$$\mathbf{P}_2 = \begin{bmatrix} \lambda_2 + \lambda_1\cos 2\phi & \lambda_1 \sin 2\phi \\ \lambda_1 \sin 2\phi & \lambda_2 - \lambda_1 \cos 2\phi. \end{bmatrix} \quad \text{and} \quad \lambda_2 = \frac{1}{2}\left(\frac{1}{EA} + \frac{1}{kGA}\right) \tag{24}$$

and λ_1 was given in Eq. (20). With this definition and by using Eq. (2), the current coordinate of the beam centroid can be found by

$$\mathbf{x}(s) = \mathbf{x}(s_0) + \int_{s_0}^{s} \mathbf{q}(\mathbf{F}, \phi) ds \tag{25}$$

Because the function $\mathbf{q}$ is entirely determined by knowledge of the orientation ϕ and applied external force $\mathbf{F}$, the integral Eq. (25) can be employed to evaluate the deformed configuration of the beam in a straightforward manner. This system reduction offers advantages when compared to the original system of Eq. (8). First, the size of the system of equations is divided by three; this means that the size of the associated computational problem will also be reduced by a factor of three. This is very attractive when a large number of fibers (beam) are considered. Further, because a single field (ϕ) is considered, there will be no numerical issues to ensure that the displacement field $\mathbf{x}$ and rotation field ϕ are compatible. This feature thus ensures a locking-free finite-element formulation.

Integral Equations for Kinematic Constraints

Although the preceding formulation provides a very efficient way to compute the finite deformation of a single beam, it cannot describe the deformation of a family of interacting beams (or fibers), such as observed in fibrous networks. This is because cross-linking (or fiber-fiber attachment) is a typical case of translational (and rotational) kinematic constraints at the intersection point between fibers. The primary contribution of this paper is thus to generalize the reduced formulation introduced in the previous section such that a variety of kinematic constraints—for instance, cross-link constraints—can be applied to a beam. This will permit the use of the efficient and reduced beam theory to the deformation of a large number of intersecting fibers. For clarity, two cases of kinematic constraints will be considered. The first case will concern a single beam along which a prescribed displacement $\bar{\mathbf{u}}$ is imposed. The second case will concern two interacting beams that are constrained to have the same displacement at their intersection point (cross-link constraint).

Fixed Translational Constraints on a Single Beam

Consider a beam for which the displacement $\mathbf{u}_j$ at $s = s^j$ is imposed ($j = 1, \ldots, n_c$ where n_c = number of translational constraints). For convenience, the coordinate of this point is introduced as $\bar{\mathbf{x}}^j = \mathbf{X}(s^j) + \bar{\mathbf{u}}^j$ such that constraint equation reads

$$\mathbf{x}(s^j) = \bar{\mathbf{x}}^j \tag{26}$$

To enforce this equation within the presented formulation, it is first useful to note that from the duality of mechanics, the stipulation of the displacements at a point is equivalent to the specification of a conjugate point force vector $\mathbf{f}^j$ at the same location. Accordingly, the problem may recast as one of finding the concentrated force $\mathbf{f}^j$ applied at point s^j such that Eq. (26) is verified. Because vector $\mathbf{q}$ is an explicit function of the external loads, Eq. (25) may be used in (26) to obtain an integral equation for $\mathbf{f}^j$ as follows:

$$\int_0^{s^j} \mathbf{q}[\mathbf{F}(\mathbf{f}^j, \phi)] ds = \bar{\mathbf{x}}^j - \mathbf{x}(0) \tag{27}$$

The problem then consists of finding the unknown force $\mathbf{f}^j$ applied at $s = s^j$ such that Eq. (27) is verified. This can be done numerically with the finite-element method, described in the section "Finite-Element Implementation."

Translational Constraints between Two Interacting Beams

The problem of interacting beams (or fibers) is very relevant to studies related to the mechanics of fibrous networks. A particular mode of interaction in networks results from the presence of cross-links that can often be modeled as rigid connections between two beams at their point of intersection. In the present model, this interaction is seen as a constraint, forcing displacements to be the same at the cross-link locations. Consider two interacting beams, denoted as A and B, whose curvilinear coordinates are s_A and s_B, respectively. According to Eq. (25), the deformed coordinates $\mathbf{x}_A$ and $\mathbf{x}_B$ of points on Beams A and B are then

$$\mathbf{x}_A(s_A) = \mathbf{x}_\mathbf{A}(0) + \int_0^{s_A} \mathbf{q}(\mathbf{F}_A, \phi_A) ds \tag{28}$$

$$\mathbf{x}_B(s_B) = \mathbf{x}_\mathbf{B}(0) + \int_0^{s_B} \mathbf{q}(\mathbf{F}_B, \phi_B) ds \tag{29}$$

where the subscripts A and B are used to designate quantities associated to Beams A and B. Now consider a number n_{cl} of cross-links ($j = n_c + 1, \ldots, n_c + n_{cl}$), bridging Beams A and B at locations s^j_A and s^j_B on Beams A and B, respectively. Because the cross-link location is given by intersection points between fibers

$$\mathbf{X}_A(s_A^j) = \mathbf{X}_B(s_B^j) \tag{30}$$

where $\mathbf{X}_A$ and $\mathbf{X}_B$ = coordinates of the undeformed beams in the global Cartesian coordinate system. Because for rigid cross-links the relative displacement of the two beams at the cross-link should vanish, their current coordinates $\mathbf{x}_A$ and $\mathbf{x}_B$ verify

$$\mathbf{x}_A\left(s_A^j\right) = \mathbf{x}_B\left(s_B^j\right) \tag{31}$$

Similar to what is done for a fixed constraint, applying constraint (31) is equivalent to applying a concentrated force on each beam. Further, from the principle of action and reaction, the forces on each beam should be of equal magnitude and opposite direction. Thus a concentrated cross-link force $\mathbf{f}^j$ is introduced such that $\mathbf{f}^j$ is applied on Beam A at $s_A = s_A^j$, and $-\mathbf{f}^j$ is applied on Beam B at $s_B = s_B^j$. Using Eqs. (28), (29), and (31), the force $\mathbf{f}^j$ can be determined from the following constraint equation:

$$\int_0^{s_A^j} \mathbf{q}[\phi_A, \mathbf{F}_A(\mathbf{f}^j)]ds - \int_0^{s_B^j} \mathbf{q}[\phi_B, \mathbf{F}_B(-\mathbf{f}^j)]ds = \mathbf{x_B}(0) - \mathbf{x_A}(0) \tag{32}$$

Once again, the concentrated force $\mathbf{f}^j$ can be determined numerically with the finite-element method.

Summary of the Reduced Beam Formulation with Kinematic Constraints

To be complete, this section provides a summary of the formulation for the reduced beam formulation with translational constraints. Considering beams subject to loading conditions defined by $\mathbf{F}$ [Eq. (17)] and subjected to fixed and cross-link displacement constraints, the problem consists of finding the orientation $\phi(s)$ of the beam axis and forces $\mathbf{f}^j$, conjugate to kinematic constraints, by solving the following three coupled equations:

Moment equation

$$EI(\phi' - \phi_0') + g(\mathbf{F}, \phi) = 0 \qquad \text{on } (0, L) - \{s^j\} \tag{33}$$

Fixed displacement constraint at $s = s^j$

$$\int_0^{s^j} \mathbf{q}(\phi, \mathbf{F}(\mathbf{f}^j))ds = \bar{\mathbf{x}}^j - \mathbf{x}(0) \tag{34}$$

Cross-link displacement constraint at $s = s_A^j$ (Beam A) and $s = s_B^j$ (Beam B)

$$\int_0^{s_A^j} \mathbf{q}[\phi_A, \mathbf{F}_A(\mathbf{f}^j)]ds - \int_0^{s_B^j} \mathbf{q}[\phi_B, \mathbf{F}_B(-\mathbf{f}^j)]ds = \mathbf{x_B}(0) - \mathbf{x_A}(0) \tag{35}$$

In addition to these translational constraints, other conditions can be imposed on the beam rotation to describe (1) concentrated moments, (2) fixed rotation constraint, or (3) cross-link rotation constraint. These can be summarized as follows:

Concentrated moment $\bar{M}^j$

$$EI(\phi' - \phi_0')(s^j) = \bar{M}^j \tag{36}$$

Fixed rotation $\bar{\phi}^j$ constraint at $s = s^j$

$$\phi(s^j) = \bar{\phi}^j \tag{37}$$

Cross-link rotation constraint at $s = s_A^j$ (Beam A) and $s = s_B^j$ (Beam B)

$$\phi(s_A^j) = \phi(s_B^j) \tag{38}$$

Once the beam orientation ϕ and the constraint force $\mathbf{f}^j$ are obtained, the coordinate of point $\mathbf{x}$ along the beam in the deformed configuration may be computed by using Eq. (25). This formulation retains the advantages of the reduced beam equation while incorporating constraints that are important for a large variety of problems. In terms of the number of unknowns, in two dimensions, only two additional unknowns (components of $\mathbf{f}^j$) are added to the system for each translational constraint. This constitutes a significant reduction compared to the original problem [Eq. (8)].

Finite-Element Implementation

For a general solution, a basic 1D finite-element procedure is now presented. For clarity and simplicity, a linear approximation of the rotation field is considered.

Finite-Element Discretization and Implementation

Proceeding to the finite-element discretization, the beam shown in Fig. 2 is subdivided in n_e elements of length ℓ_e. The rotation field ϕ is represented by a vector $\{\Phi\}$ whose component Φ_I denotes the value of the rotation at node I. For the eth two-node linear element, the element rotation vector may be written as

$$\Phi^e = \begin{Bmatrix} \Phi_1^e \\ \Phi_2^e \end{Bmatrix} \tag{39}$$

whose components represent the values of ϕ associated with nodes that belong to the eth element (whose corresponding fields are represented by the superscript e). Within the eth element, an approximation $\tilde{\phi}$ of the rotation ϕ is written in terms of interpolation of the nodal values Φ^e as follows:

$$\tilde{\phi}^e(\xi) = \mathbf{N}(\xi)\Phi^e \quad \text{with } \mathbf{N} = \begin{bmatrix} \frac{1-\xi}{2} & \frac{\xi+1}{2} \end{bmatrix} \tag{40}$$

where $\mathbf{N}$ = finite-element shape functions; and ξ $(-1 \le \xi \le 1)$ = local coordinate in a system associated with an element. Accordingly, the derivative of $\tilde{\phi}^e$ with respect to the curvilinear coordinate s is constant and may be written in terms of a vector $\mathbf{B}$ as

$$\tilde{\phi}_{,s}^e(\xi) = \mathbf{B}(\xi)\Phi^e \quad \text{where } \mathbf{B} = \frac{2}{\ell_e}\frac{d\mathbf{N}}{d\xi} = \begin{bmatrix} -\frac{1}{\ell_e} & \frac{1}{\ell_e} \end{bmatrix} \tag{41}$$

Discretization of Moment Differential Equation

For a finite-element discretization of Eq. (21), a weak form may first be derived by premultiplying it by a test function ψ and integrating over the initial length. This yields

$$\int_0^L \frac{d[EI(\phi - \phi_0)]}{ds}\frac{d\psi}{ds} - g(\phi, \mathbf{f}_i)\psi)ds - \sum_{j=1}^{n}[m^j\psi]_{s=s^j} = 0 \tag{42}$$

with $[EI(\phi - \phi_0)]_{s=s^j} = m^j$. Interpolating the test function ψ with the same shape functions as those used for interpolating ϕ, the finite-element approximation of Eqs. (40) and (41) may be substituted into Eq. (42) to find

$$\sum_{e=1}^{n_e}(\Psi^e)^T\frac{\ell_e}{2}\left[\left(\int_{-1}^{1} EI\mathbf{B}^T\mathbf{B}d\xi\right)(\Phi^e - \Phi_0^e) - \int_{-1}^{1}\mathbf{N}^T g d\xi - \mathbf{P}\mathbf{m}^e\right] = 0 \tag{43}$$

J. Eng. Mech., 2011, 137(8): 527-536

where Ψ^e = nodal values of the test function in element e; and $\mathbf{m}^e = [m_1^e \quad m_2^e]^T$ = vector whose components give the value of the concentrated moment at nodes of element e. The vector $\mathbf{P}$ is defined by

$$\mathbf{P} = \begin{cases} [1 \quad 1/2] & \text{if } e = 1 \\ [1/2 \quad 1/2] & \text{if } e = n_e \\ [1/2 \quad 1] & \text{otherwise} \end{cases} \tag{44}$$

with the requirement that the forgoing equality holds for any arbitrary vector Ψ^e, this leads to a matrix equation for Φ^e as

$$\mathbf{K}^e(\Phi^e - \Phi_0^e) - \mathbf{G}^e = \mathbf{0} \tag{45}$$

where the element stiffness matrix $\mathbf{K}^e$ and the vector $\mathbf{G^e}$ are given by

$$\mathbf{K}^e = \frac{\ell_e}{2}\int_{-1}^{1} EI\mathbf{B}^T\mathbf{B}d\xi \tag{46}$$

$$\mathbf{G}^e = \frac{\ell_e}{2}\int_{-1}^{1} \mathbf{N}^T g d\xi - \mathbf{P}\mathbf{m}^e \tag{47}$$

Combining the preceding elemental equations into a global system of equations by standard finite-element assembly procedures results in

$$\mathbf{H}_1(\Phi, \mathbf{f}^j) = \mathbf{K}(\Phi - \Phi_0) - \mathbf{G}(\Phi, \mathbf{f}^j) = \mathbf{0} \tag{48}$$

where $\mathbf{K}$ and $\mathbf{G}$ = assembled global stiffness matrix and force vector, and the unknown rotation vector Φ and concentrated force $\mathbf{f}^j$ at prescribed nodes are explicitly displayed for the sake of clarity.

Integral Equation for Constrained Displacements

For problems involving prescribed pointwise displacements, the integral Eq. (27) can be rewritten in terms of nodal rotation and distributed forces by means of Eqs. (40) and (41). An elemental expression of $\tilde{\mathbf{q}}^e$ for the function $\mathbf{q}$ may, for instance, be computed in terms of $\tilde{\phi}^e$. In the context of the proposed linear finite-element approximation, the integral equation $\mathbf{H}_2^j$ corresponding to the application of a prescribed displacement at node $s = s^j$ can be written as a summation of contributions from various elements, as in

$$\mathbf{H}_2^j(\Phi, \mathbf{f}^j) = \sum_{e=1}^{n_j}\left[\frac{\ell_e}{2}\int_{-1}^{1}\tilde{\mathbf{q}}^e(\Phi, \mathbf{f}^j)d\xi\right] - [\bar{\mathbf{x}}^j - \mathbf{x}(s_0)] = \mathbf{0} \tag{49}$$

where n_j = number of elements between $s = 0$ and the node located at $s = s^j$ (at which the prescribed displacement is applied). To account for cross-link displacement constraints, a vector $\mathbf{H}_3^j$ can also be introduced in the form

$$\mathbf{H}_3^j(\Phi, \mathbf{f}^j) = \sum_{e=n_A^1}^{n_A^j}\left[\frac{\ell_e}{2}\int_{-1}^{1}\tilde{\mathbf{q}}^e(\Phi, \mathbf{f}^j)d\xi\right] - \sum_{e=n_B^1}^{n_B^j}\left[\frac{\ell_e}{2}\int_{-1}^{1}\tilde{\mathbf{q}}^e(\Phi, \mathbf{f}^j)d\xi\right] - [\mathbf{x}_B(0) - \mathbf{x}_A(0)] = \mathbf{0} \tag{50}$$

where n_A^1 and n_B^1 = number of the first elements of Beams A and B, respectively; and n_A^j and n_B^j = number of elements whose second node is located at $s = s_A^j$ and $s = s_B^j$, respectively. Although the integrals appearing in Eqs. (49) and (50) may be calculated analytically in closed form, as discussed in Pak and Stauffer (1994), it is found to be computationally efficient to employ normal Gaussian quadrature. Assembling the contributions from all nodes at which the displacement is prescribed, two vectors are obtained, corresponding to fixed and cross-linked displacement constraints, respectively

$$\mathbf{H}_2(\Phi, \mathbf{f}^j) = \begin{bmatrix} \mathbf{H}_2^1(\Phi, \mathbf{f}^j) \\ \vdots \\ \mathbf{H}_2^m(\Phi, \mathbf{f}^j) \end{bmatrix} = \mathbf{0} \quad \text{and} \qquad \mathbf{H}_3(\Phi, \mathbf{f}^j) = \begin{bmatrix} \mathbf{H}_3^1(\Phi, \mathbf{f}^j) \\ \vdots \\ \mathbf{H}_3^n(\Phi, \mathbf{f}^j) \end{bmatrix} = \mathbf{0} \tag{51}$$

Nonlinear Solution of the Global System

In summary, the finite deformation analysis of a beam is reduced to finding the nodal rotation vector Φ and the discrete force vectors $\mathbf{f}^j$ corresponding to displacement constraints, such that

$$\mathbf{H}(\Phi, \mathbf{f}^j) = \begin{bmatrix} \mathbf{H}_1(\Phi, \mathbf{f}^j) \\ \mathbf{H}_2(\Phi, \mathbf{f}^j) \\ \mathbf{H}_3(\Phi, \mathbf{f}^j) \end{bmatrix} = \mathbf{0} \tag{52}$$

This system consists of $(n_e + 1) + 2(n_c + n_{cl})$ equations that are to be solved for an equal number of unknowns, namely the $(n + 1)$ nodal rotations and the $2(n_c + n_{cl})$ force vector components arising from applications of n_c translational constraints and the existence of n_{cl} cross-links. A solution to this nonlinear system can be numerically determined by using a Newton-Raphson procedure. Defining the variable vector $\mathbf{u} = (\Phi, \mathbf{f}^j)$, the function $\mathbf{H}^\nu$ at iteration ν is given as $\mathbf{H}^\nu = \mathbf{H}(\mathbf{u}^\nu)$. The solution $\mathbf{u}^{\nu+1}$ at the next iteration is then given by

$$\mathbf{u}^{\nu+1} = \mathbf{u}^\nu - \left[\frac{d\mathbf{H}}{d\mathbf{u}}\right]^{-1}\mathbf{H}^\nu \tag{53}$$

Iterations are repeated until the norm $|\mathbf{H}^\nu| < t$, where t = tolerance. As will be illustrated in the following section, the proposed analytical-numerical method performs extremely well, with excellent accuracy and computational efficiency for all examples considered.

Examples and Discussion

To assess the performance in terms of the efficiency and accuracy of the method, several benchmark problems are considered, each illustrating a particular aspect of the method. The first set of examples investigates the performance of the method when no kinematic constraints are present. Both cases of conservative and nonconservative forces are illustrated. The second set of examples explores a problem involving a fixed kinematic constraint, in the case of a circular arch loaded in the vertical direction. Finally, the third problem concentrates on a system of interacting beams linked by two kinds of cross-links: links with no rotational stiffness and rigid links. Then the consequences of making such assumptions on the mechanical response of the system of fibers are investigated.

Examples with No Kinematic Constraints: Cantilever Beams

Bending of a Cantilever Beam Subjected to a Follower Force

The first illustration concerns an initially straight cantilever beam of length $\ell = 100$ m subjected to an increasing follower force at its end that remains perpendicular to the centroidal axis during the process. A previous numerical solution to this problem was presented

by Argyris and Symeonides (1981) and later by Simo and Vu-Quoc (1986) with their separate displacements and rotation field approximations for the following material parameters: $EI = 3.5 \times 10^7$ N · m^2 and $GA = 1.61538 \times 10^8$ N. The solution to this problem by the proposed method with two Gauss points per element in this study is shown in Fig. 3, with a coarse (nine elements) and fine (100 elements) discretization of the single variable ϕ. The deformed configuration, plotted with a load increment of 9.3 kN up to a final load of 130 kN, and the load-deflection curves agree perfectly with the solutions derived in Argyris and Symeonides (1981) and Simo and Vu-Quoc (1986). Excellent results can be obtained with only a coarse mesh by the described formulation.

Postbuckling Analysis of a Vertical Beam Subjected to a Vertical End Force

This example investigates the postbuckling response of a straight, vertical beam of length $\ell = 40$ under the action of a conservative vertical load at its end. Because the top end is free, no constraint equations are necessary for this problem. To capture the eventual unstable behavior, the standard arc-length control (Ricks 1972) was incorporated into the algorithm and found to be effective. The beam deformation and load displacement were then computed for various discretization levels (Fig. 4). Again, good convergence to the exact solution in total agreement with the solution found in Pak and Stauffer (1994) can be achieved with minimal number of elements.

Example with Fixed Kinematic Constraints: Instability of a Circular Arch Subjected to a Top Vertical Force

This example illustrates an instability-bifurcation problem when a fixed constraint is needed. Consider a circular arch subjected to a top vertical conservative load, for which the displacements of two ends are constrained ($s = 0$ and $s = s_n$). With the aid of the arc-length control method as in the last example, Fig. 5(a) shows the deformation of the arch for various loads, and Fig. 5(b) gives the load-deflection relationship under different finite-element discretizations. In the prebuckling regime, it was found that the use of only two elements is sufficient to give good solutions comparable to those given in Knight and Carron (1997). As expected, however, as the load approaches the instability limit, the solution becomes sensitive to the number of elements. This is because high curvature

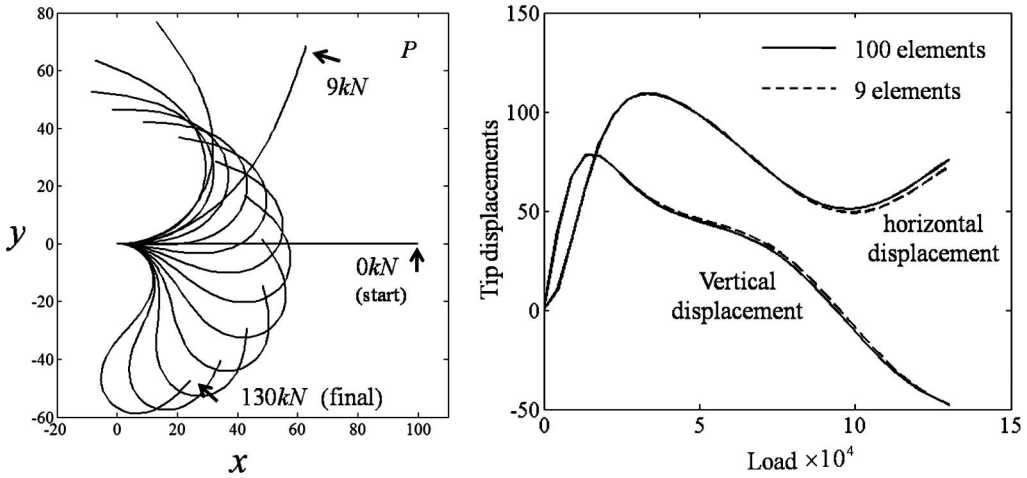

Fig. 3. Deformed configuration and structural response of a cantilever beam subjected to a follower force perpendicular to the beam cross section and applied at the end tip

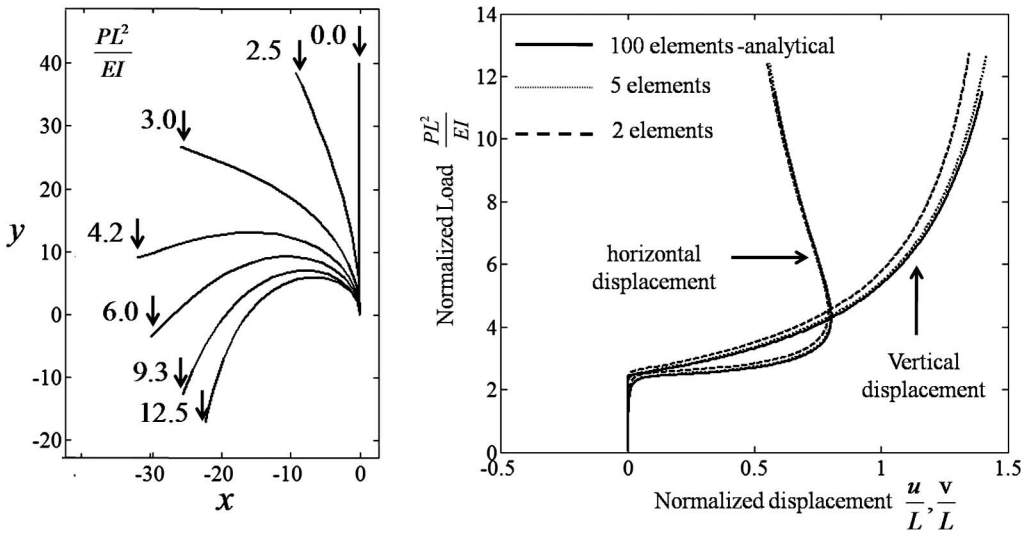

Fig. 4. Deformation of a beam in the postbuckling regime caused by the action of a vertical force applied at its top end; normalized force-displacement response

J. Eng. Mech., 2011, 137(8): 527-536

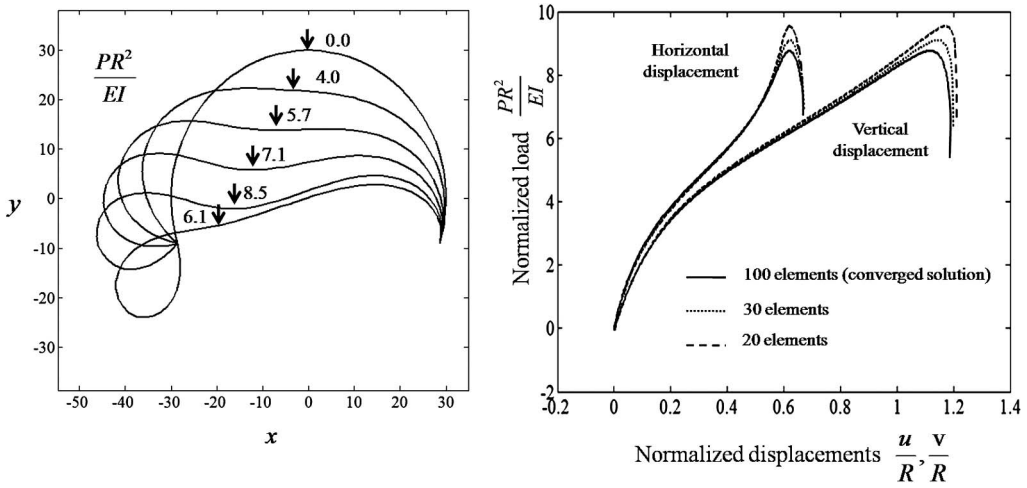

Fig. 5. Deformation and force-displacement response of an arch undergoing instability because of the action of a vertical force

variations develop during and after the instability. As a result, it is natural that a finer discretization is needed to capture the higher gradient of deformation.

Examples with Cross-Link Constraints: Extension of Multifiber Systems

This example uses some applications of the cross-linked constraint method introduced in this paper and investigates the effect of cross-link constraints and a set of interacting sinusoidal fibers. In particular, the example assesses the effect of two types of cross-link constraints: (1) links with rotational rigidity, and (2) links with no rotational rigidity. For links with rotational rigidity, both displacements and rotation are prescribed at the link, and for links with no rotational rigidity, only displacements are prescribed.

Stretching of a Single Sinusoidal Fiber

Before introducing the cross-linked system, it is useful to assess the behavior of a single sinusoidal fiber under extension. The fiber under investigation is a sinusoidal-shaped slender beam of length 1 m with a circular cross section of radius $r = 0.005$ m, Young's modulus $E = 1{,}000$ Pa, and shear modulus $G = 400$ Pa. The fiber is extended by constraining its right end to undergo a horizontal displacement $d = 0.2$ m and no vertical displacement (Fig. 6). As expected, the force-extension relation for the fiber exhibits a stiffening in its response as the fiber straightens (Fig. 6). For this example, convergence was obtained for 20 elements because of the high initial curvature. In the next three examples, 30 elements were used.

Stretching of Two Interacting Sinusoidal Fibers

To understand the effect of cross-link constraints, now the interaction of two fibers with the same properties and geometry as that described previously is considered. Keeping the original fiber in the same configuration as previously, the second is translated to the right by an amount of half the fiber's wavelength. Cross-link constraints are then specified at three locations, corresponding to intersection points between the two fibers. Fiber stretching is obtained by prescribing similar boundary conditions to those used

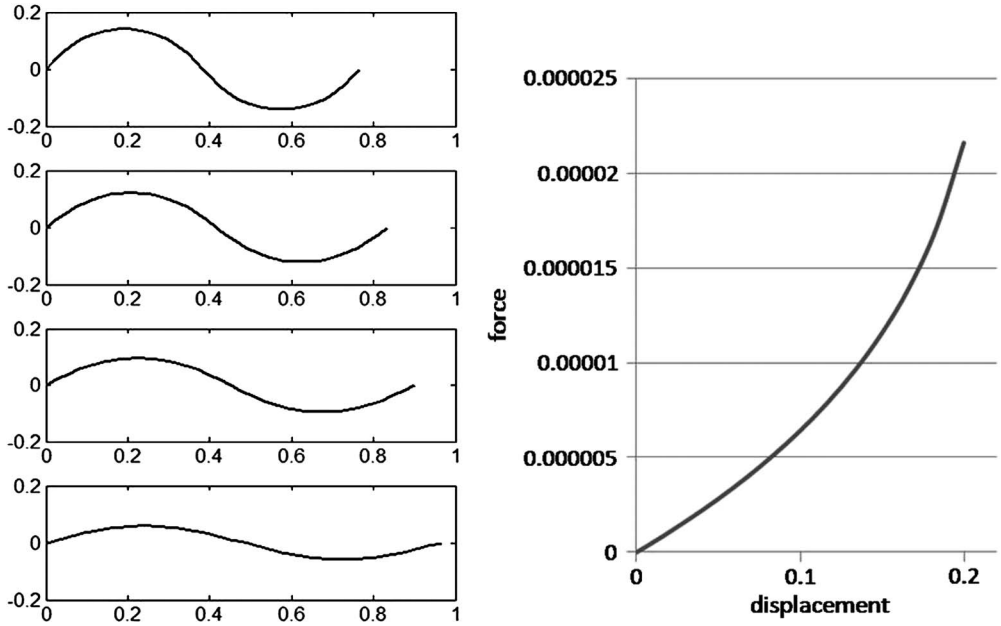

Fig. 6. Stretching of a single sinusoidal fiber and resulting force-displacement behavior

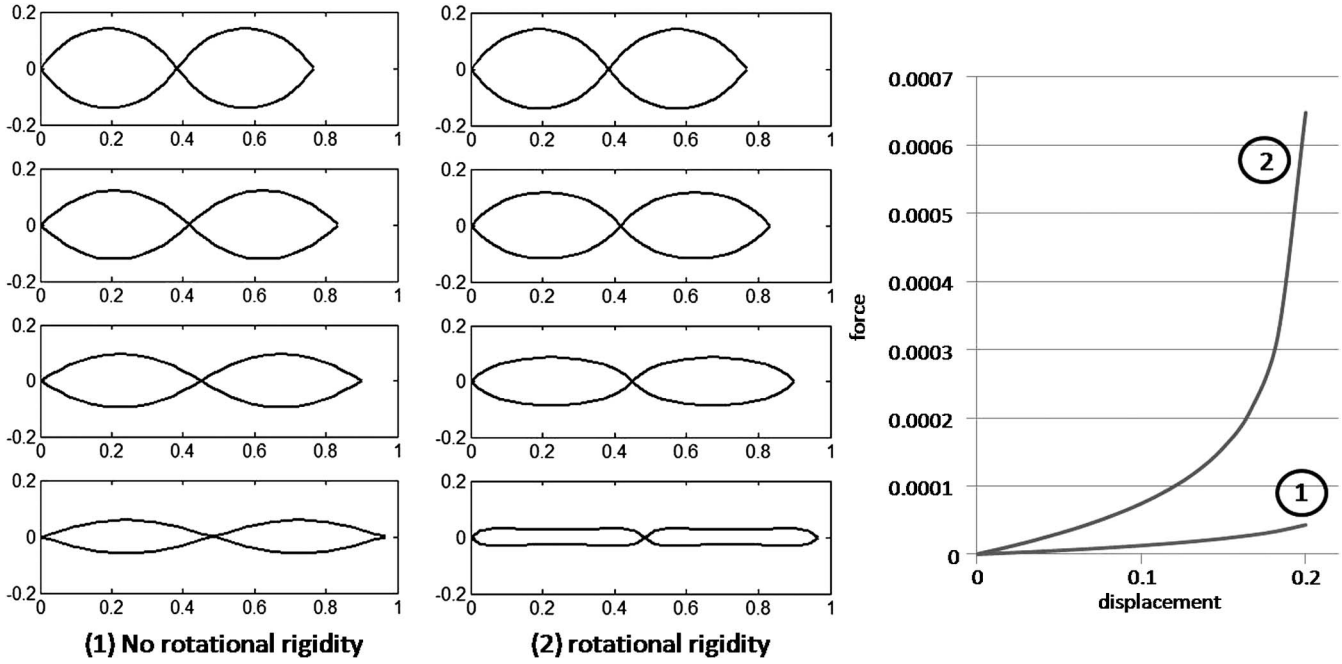

Fig. 7. Stretching of a system of two interacting sinusoidal fibers and resulting force-displacement behavior

previously and deformed configurations are given in Fig. 7 for four extension values: $e = 0$, $e = 0.07$, $e = 0.14$, and $e = 0.2$. Two distinct behaviors are obtained according to cross-link type. When the cross-link has no rotational rigidity, there are no effects from cross-links on fiber deformation. The resulting force-extension response is therefore characterized by a curve similar to Fig. 6, with double the stiffness (because two fibers are present). The scale used for the stress-strain diagrams is different in Figs. 6 and 7. However, when constraints with rotational rigidity are considered, the angle between fibers remains constant during deformation, forcing the fiber to undergo a more severe deformation. The consequence of this is an increased stiffness and stiffening of the curve in Fig. 7. This example emphasizes the importance of cross-links behavior on multifiber systems. The high fiber curvature near cross-links when cross-links have rotational rigidity implies that more elements must be used in the concerned regions. Although manual refinement was done in this work, general adaptive refinement methods can be used to maximize accuracy while maintaining computational efficiency.

Stretching of Three Interacting Sinusoidal Fibers

This final example investigates the tensile mechanical response of a strand of three interacting sinusoidal fibers with different cross-link

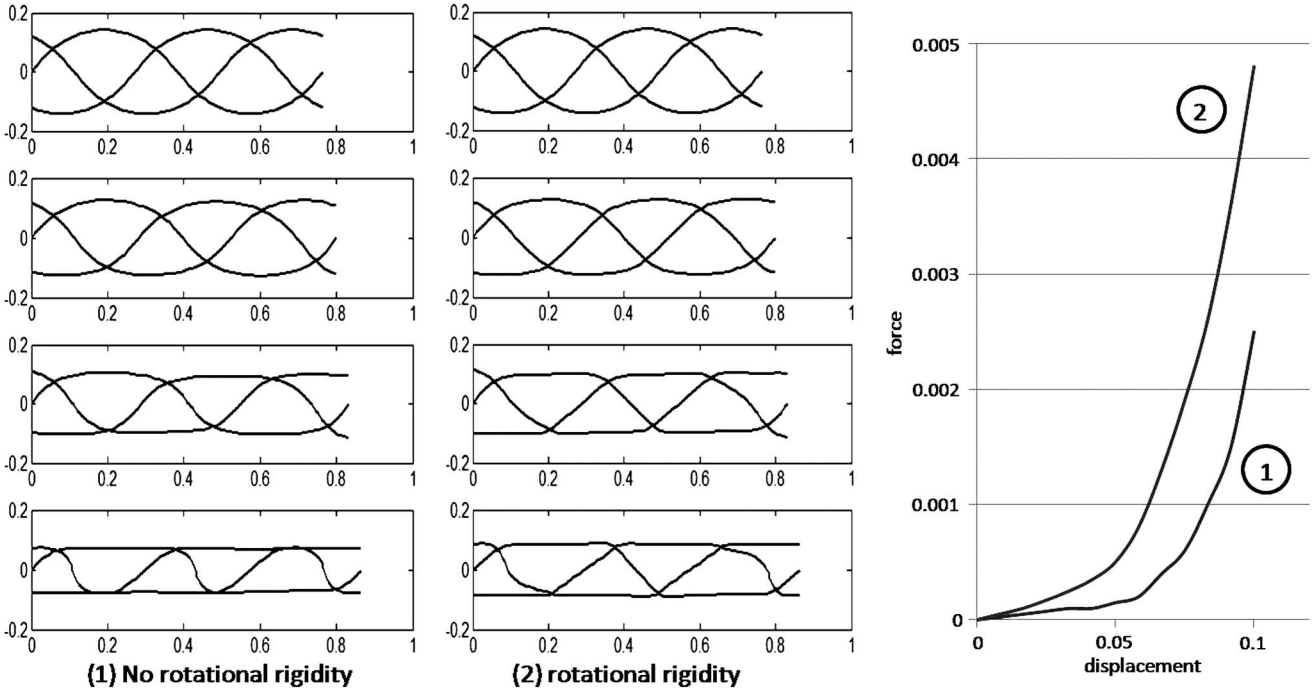

Fig. 8. Stretching of a system of three interacting sinusoidal fibers and resulting force-displacement behavior

J. Eng. Mech., 2011, 137(8): 527-536

constraints. The geometry of the strand is characterized by the original sinusoidal fiber and two additional fibers, each offset by an amount of one-third of the fiber's wavelength (Fig. 8). Once again, cross-links are located at the fiber's intersection points (six cross-links are present here). For this example, a stretch of $d = 0.1$ m is applied in the horizontal direction, leading to the deformed configurations displayed in Fig. 8. With this configuration, even when there is no rotational rigidity, constraints impede the free deformation of fibers, and in the final configuration, only certain fiber segments are fully stretched. These segments are the principal contributors to the mechanical response of the multifiber system. This phenomenon is observed for both types of cross-links, which explains the relatively minor difference in force-extension response between the two systems. However, once again, a larger stiffness is obtained when cross-links are rigid.

Conclusion

This paper presents a hybrid analytical–computational mechanics formulation for an arbitrarily curved beam undergoing large planar displacements and rotation, and kinematic constraints. By analytically eliminating the governing equations involving axial and shear resultants in the 1D theory, it is shown that the set of field equations can be reduced to a single nonlinear ordinary differential equation on the cross-sectional rotation angle. To apply translational kinematic constraints, an integral equation relating external forces, beam orientation, and specified displacements is employed and implemented computationally. Because the formulation has only one primary unknown, the analytical framework leads to a numerical problem whose size is one-third of those using three-field (two translational and a rotational degree of freedom at each node) discretizations. This reduction in problem size and discretization error leads to excellent numerical performance of the method, rendering it an attractive platform for the multiscale computational homogenization, as in Vernerey et al. (2007, 2008) of soft fibrous materials, in which a large number of fibers is present. As a result, the presented formulation should be useful in obtaining solutions of high accuracy to serve as benchmarks for research in biomechanics, structural mechanics, wire meshes and nets, woven materials, and many related modern engineering applications.

References

Argyris, J., and Symeonides, S. (1981). "Nonlinear finite element analysis of elastic systems under nonconservative loading—Natural configuration. Part 1. Quasistatic problems." *Comput. Methods Appl. Mech. Eng.*, 26, 373–383.

DaDeppo, D., and Schmidt, R. (1969). "Sidesway buckling of deep circular arches under a concentrated load." *J. Appl. Mech.*, 36(2), 325–327.

Goto, Y., Yoshimitsu, T., and Obata, M. (1990). "Eliptic integral solutions of plane elastica with axial and shear deformation." *Int. J. Solids Struct.*, 26(4), 375–390.

Huddleston, J. (1968). "Finite deflections and snapthrough of high circular arches." *J. Appl. Mech.*, 35(4), 763–769.

Irschik, H., and Gerstmayr, J. (2009). "A continuum mechanics based derivation of Reissner's large-displacement finite-strain beam theory: The case of plane deformations of originally straight Bernoulli-Euler beams." *Acta Mech.*, 206(1–2), 1–21.

Kapania, R. (1986). "A formulation and implementation of geometrically exact curved beam elements incorporating finite strains and finite rotations." *Comput. Methods Appl. Mech. Eng.*, 49, 55–70.

Knight, N., and Carron, W. S. (1997). "Statics collapse of elastic arches." *AIAA J.*, 35(12), 1876–1880.

Lau, G. (1982). "Large deflection of beams with combined loads." *J. Eng. Mech.*, 108(1), 180–185.

Pak, R., and Stauffer, E. (1994). "Nonlinear finite deformation analysis of beams and colunms." *J. Eng. Mech.*, 120(10), 2136–2153.

Ricks, E. (1972). "The application of Newton's method to the problem of elastic stability." *J. Appl. Mech.*, 39(4), 1060–1065.

Saje, M. (1990). "A variational principle for finite planar deformation of straight slender elastic beams." *Int. J. Solids Struct.*, 26(8), 887–900.

Saje, M. (1991). "Finite element formulation of finite planar deformation of curved elastic beams." *Comput. Struct.*, 39(3–4), 327–337.

Schmidt, R., and DaDeppo, D. (1972). "Buckling of clamped circular arches subjected to a point load." *J. Appl. Math. Phys. (1950-1981)*, 23, 146.

Simo, J. (1985). "A finite strain beam formulation. The three dimensional dynamic problem. Part 1." *Comput. Methods Appl. Mech. Eng.*, 49, 55–70.

Simo, J., and Vu-Quoc, L. (1986). "A three dimensional finite strain rod model. Part II: Computational aspects." *Comput. Methods Appl. Mech. Eng.*, 58, 79–116.

Vernerey, F., Liu, W., and Moran, B. (2007). "Multiscale micromorphic theory for hierarchical materials." *J. Mech. Phys. Solids*, 55(12), 2603–2651.

Vernerey, F., Liu, W., Moran, B., and Olson, G. (2008). "A micromorphic model for the multiple scale failure of heterogeneous materials." *J. Mech. Phys. Solids*, 56(4), 1320–1347.

J. Eng. Mech., 2011, 137(8): 527-536